Réduction de modèles et analyse de sensibilité appliqué à un modèle biophysique dans l'œil humain

Thomas Saigre

Séminaire doctorant IRMA
15th June 2023

Introduction

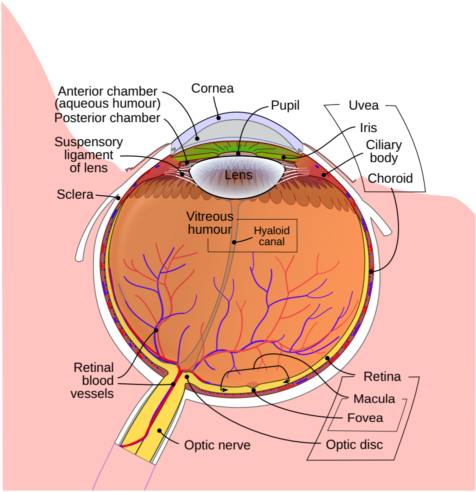

Rhcastilhos, from Wikipedia

- Need to understand ocular **physiology** and **pathology**,
- **Heat transfer** has an impact on the distribution of drugs in the eye [a],
- Complexity to perform **measurements** on a human subject [b], only on surface [c].

[a] Bhandari et al., J. Control Release (2020)
[b] Rosenbluth et al., Exp. Eye Res. (1977)
[c] Purslow et al., Eye Contact Lens (2005)

Introduction

Model complexity

- Monophysics-Multiphysics problem
- Numerous parameters and scarce experimental data
- Influence of multiple risk factors or a combination of them

Introduction

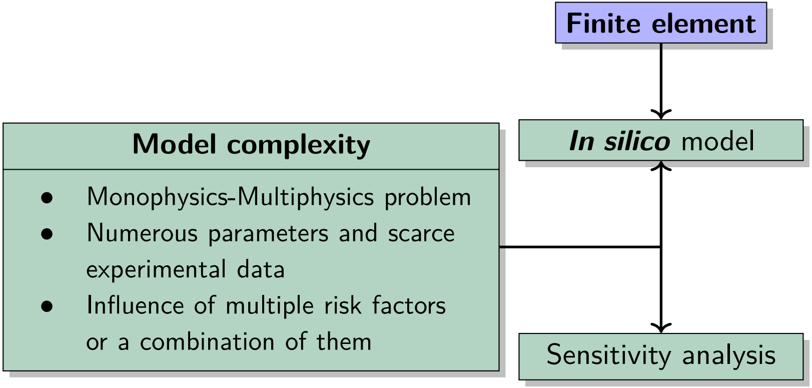

Introduction

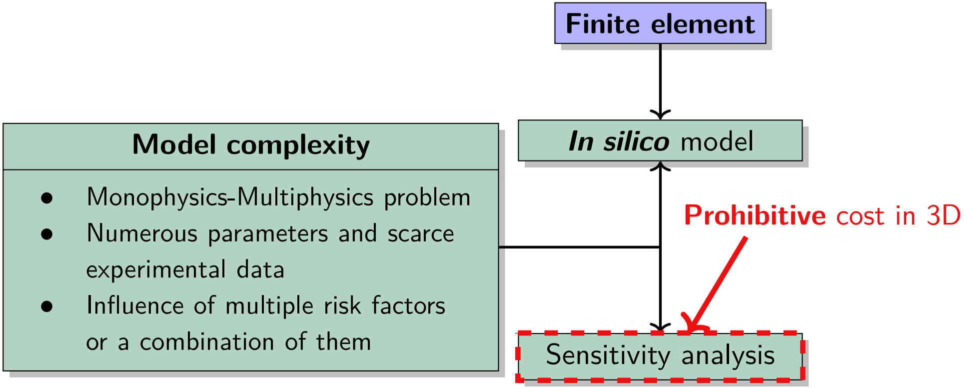

Introduction

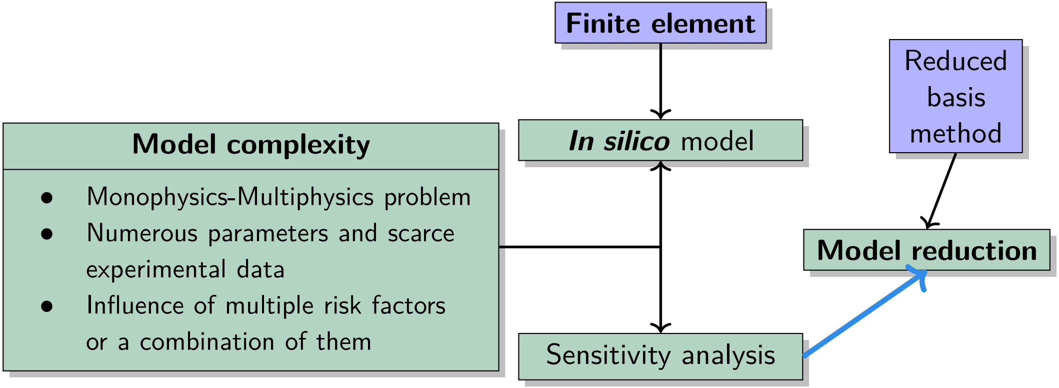

Geometrical model[1]

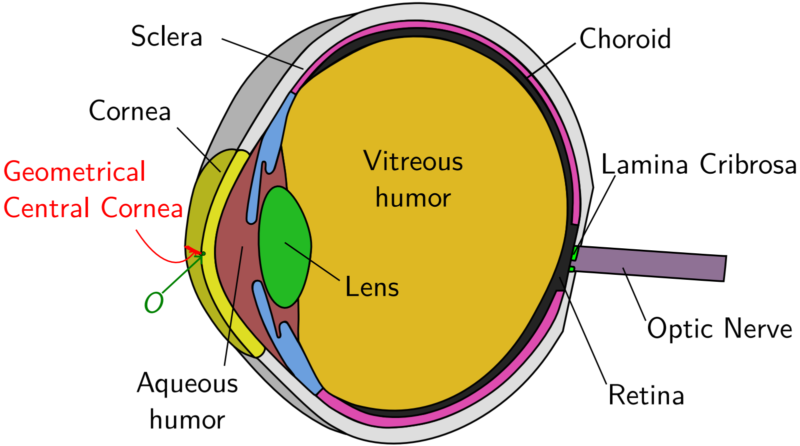

[1] Lorenzo Sala. "Mathematical modelling and simulation of ocular blood flows and their interactions". PhD Theses. Université de Strasbourg, Sept. 2019.

Biophysical model[2]

$$\rho_i C_{p,i} \frac{\partial T_i}{\partial t} + \nabla \cdot (k_i \nabla T_i) = 0 \qquad \text{over } \Omega_i$$

where :

- i is the region index (Cornea, Aqueous Humor, Vitreous Humor, Sclera, Iris, Lens, Choroid, Lamina, Retine, Optic Nerve),
- T_i [K] is the temperature in the volume i,
- t [s] is the time,
- k_i $[\mathrm{W\,m^{-1}}K^{-1}]$ is the thermal conductivity, ρ_i $[\mathrm{kg\,m^{-3}}]$ is the density and $C_{p,i}$ $[\mathrm{J\,kg^{-1}}K^{-1}]$ is the specific heat.

[2] J.A. Scott. "A finite element model of heat transport in the human eye". In: *Physics in Medicine and Biology* 33.2 (1988), pp. 227–242; Ng, E.Y.K. and Ooi, E.H. "FEM simulation of the eye structure with bioheat analysis". In: *Computer Methods and Programs in Biomedicine* 82.3 (2006), pp. 268–276.

Biophysical model

Interface conditions : $\begin{cases} T_i = T_j \\ k_i(\nabla T_i \cdot \boldsymbol{n}_i) = -k_j(\nabla T_j \cdot \boldsymbol{n}_j) \end{cases}$ over $\partial\Omega_i \cap \partial\Omega_j$

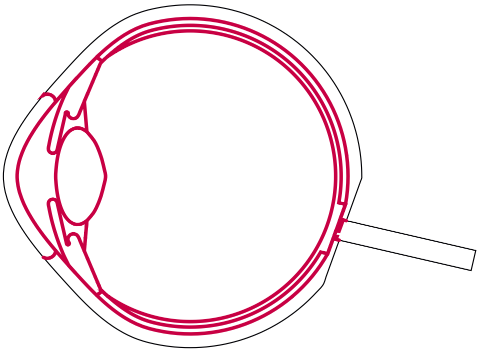

Figure 1: Description of the boundary and interface conditions of the domain

Biophysical model

Robin condition on Γ_{body} : $-k\dfrac{\partial T}{\partial \boldsymbol{n}} = h_{\text{bl}}(T - T_{\text{bl}})$

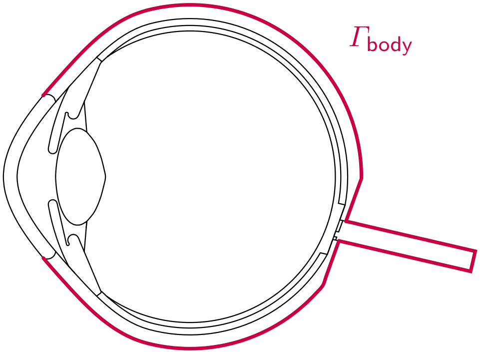

Figure 1: Description of the boundary and interface conditions of the domain

Biophysical model

Linearized Neumann condition[a] on $\varGamma_{\text{amb}}$: $-k_i \dfrac{\partial T_i}{\partial \boldsymbol{n}} = h_{\text{amb}}(T_i - T_{\text{amb}}) + h_r(T_i - T_{\text{amb}}) + E$

$h_r = 6\,\text{Wm}^{-2}\text{K}^{-1}$

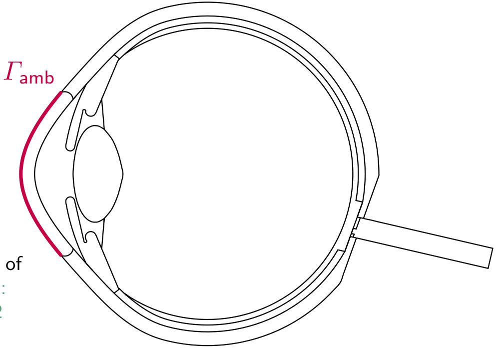

$\longrightarrow$ Model $\mathcal{E}_{\text{lin}}$

[a] J.A. Scott. "A finite element model of heat transport in the human eye". In: *Physics in Medicine and Biology* 33.2 (1988), pp. 227–242

Figure 1: Description of the boundary and interface conditions of the domain

Parameter dependant model

Symbol	Name	Dimension	baseline value
T_{amb}	Ambient temperature	[K]	298
T_{bl}	Blood temperature	[K]	310
h_{amb}	Ambiant air convection coefficient	$[\mathrm{W\,m^{-2}K^{-1}}]$	10
h_{bl}	Blood convection coefficient	$[\mathrm{W\,m^{-2}K^{-1}}]$	65
E	Evaporation rate	$[\mathrm{W\,m^{-2}}]$	40
k_{lens}	Lens conductivity	$[\mathrm{W\,m^{-1}K^{-1}}]$	0.4
k_{cornea}	Cornea conductivity	$[\mathrm{W\,m^{-1}K^{-1}}]$	0.58
k_{sclera}	Sclera conductivity	$[\mathrm{W\,m^{-1}K^{-1}}]$	1.0042
$k_{\text{AqueousHumor}}$	Aqueous humor conductivity	$[\mathrm{W\,m^{-1}K^{-1}}]$	0.28
$k_{\text{VitreousHumor}}$	Vitreous humor conductivity	$[\mathrm{W\,m^{-1}K^{-1}}]$	0.603
ε	Emissivity of the cornea	[–]	0.975

Table 1: Parameters involved in the model

Geometrical parameters may be involved, but we will not consider them in this work.

Present work : focus on parameteric analysis

Parameter	Minimal value	Maximal value	Baseline value	Dimension
T_{amb}	283.15	303.15	298	[K]
T_{bl}	308.3	312	310	[K]
h_{amb}	8	100	10	$[\mathrm{W\,m^{-2}}K^{-1}]$
h_{bl}	50	110	65	$[\mathrm{W\,m^{-2}}K^{-1}]$
E	20	320	40	$[\mathrm{W\,m^{-2}}]$
k_{lens}	0.21	0.544	0.4	$[\mathrm{W\,m^{-1}}K^{-1}]$

Table 2: Range of values for the parameters

- We set $\mu = (T_{\text{amb}}, T_{\text{bl}}, h_{\text{amb}}, h_{\text{bl}}, E, k_{\text{lens}}) \in D^{\mu} \subset \mathbb{R}^6$.
- $\bar{\mu} \in D^{\mu}$ is the baseline value of the parameters.

Reduced Basis Method

Model Order Reduction

- **Goal :** replicate input-output behavior of the high fidelity model $\mathcal{E}_{\text{full}}$ with a reduced order model $\mathcal{E}_{\text{RBM}}$,
- With a procedure stable and efficient.

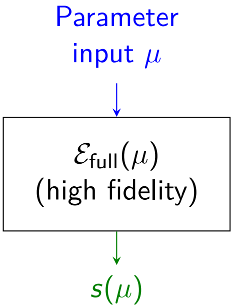

Model Order Reduction

- **Goal :** replicate input-output behavior of the high fidelity model $\mathcal{E}_{\text{full}}$ with a reduced order model $\mathcal{E}_{\text{RBM}}$,
- With a procedure stable and efficient.

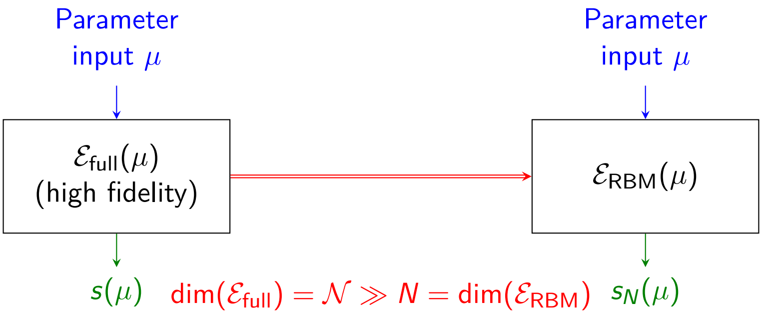

Problem statement

Problem considered

Given $\mu \in D^\mu$, evaluate the output of interest

$$s(\mu) = \ell(u(\mu); \mu)$$

where $u(\mu) \in X$ is the solution of

$$a(u(\mu), v; \mu) = f(v; \mu) \quad \forall v \in X$$

Definition

The problem is said to be *compliant* if the bilinear form a is symmetric, and $\ell = f$.

Definition

- Constant of continuity of $a(\cdot, \cdot; \mu)$: $\gamma(\mu)$
- Constant of coercivity of $a(\cdot, \cdot; \mu)$: $\alpha(\mu)$

Finite Element resolution

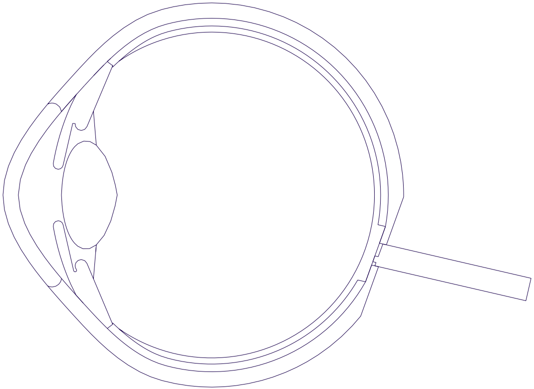

Finite Element resolution

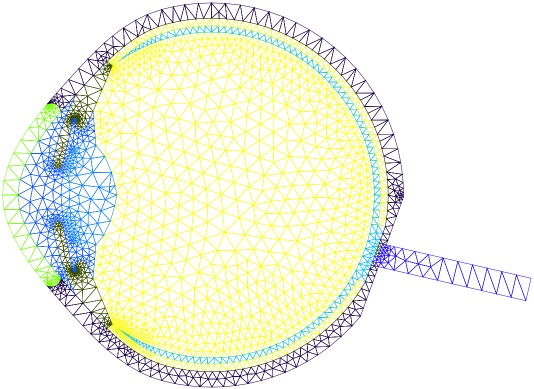

Finite Element resolution

Problem considered

Given $\mu \in D^\mu$, evaluate the output of interest

$$s(\mu) = \boldsymbol{\mathcal{L}}(\mu)^T \boldsymbol{u}(\mu)$$

where $\boldsymbol{u}(\mu) \in X^{\mathcal{N}}$ is the solution of

$$\underline{\underline{\boldsymbol{A}}}(\mu)\boldsymbol{u}(\mu) = \boldsymbol{F}(\mu)$$

Finite Element results

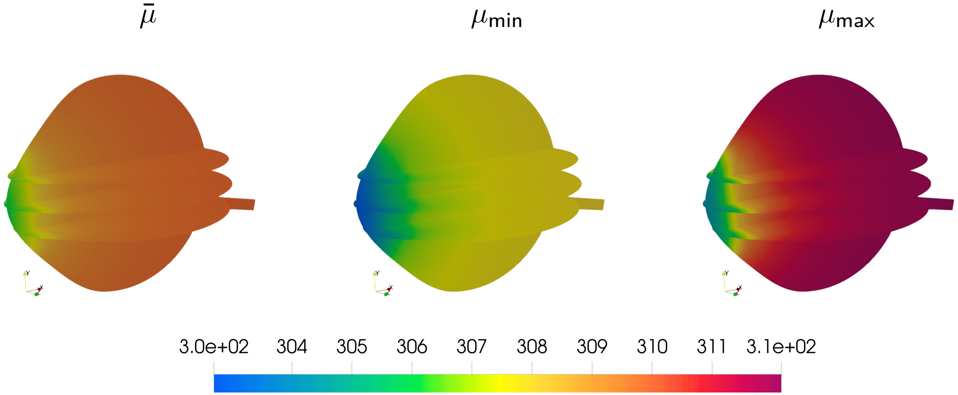

Figure 2: Distribution of the temperature [K] in the eyeball from the linear model $\mathcal{E}_{\text{L}}(\mu)$

Affine decomposition

- We want to write $\underline{\underline{\boldsymbol{A}}}(\mu) = \sum_{q=1}^{Q_a} \beta_A^q(\mu) \underline{\underline{\boldsymbol{A}}}^q$, and $\boldsymbol{F}(\mu) = \sum_{q=1}^{Q_f} \beta_F^q(\mu) \boldsymbol{F}^q$.
- Compute and store $\underline{\underline{\boldsymbol{A}}}_N^q = \underbrace{\mathbb{Z}_N^T \underline{\underline{\boldsymbol{A}}}^q \mathbb{Z}_N}_{\text{independent of } \mu}$ and $\boldsymbol{F}_N^q = \mathbb{Z}_N^T \boldsymbol{F}^q$.
- We have $Q_a = 3$ and $Q_f = 2$.

Offline / Online procedure

Offline:

- Solve N FEM systems depending on $\mathcal{N}$ to form $\mathbb{Z}_N$,
- Form and store $\boldsymbol{F}_N^p(\zeta_i)$
- Form and store $\underline{\underline{\boldsymbol{A}}}_N^q(\zeta_i)$

Online: independant of $\mathcal{N}$

Given a new parameter $\mu \in D^\mu$,

- Form $\underline{\underline{\boldsymbol{A}}}_N(\mu)$: $O(Q_a N^2)$,
- Form $\boldsymbol{F}_N(\mu)$: $O(Q_f N)$,
- Solve $\underline{\underline{\boldsymbol{A}}}_N(\mu)\boldsymbol{u}_N(\mu) = \boldsymbol{F}_N(\mu)$: $O(N^3)$,
- Compute $s_N(\mu) = \boldsymbol{\mathcal{L}}_N(\mu)^T \boldsymbol{u}_N(\mu)$: $O(N)$.

Time of execution

	Finite element resolution			Online
	$\mathbb{P}_1$	$\mathbb{P}_2$ (np=1)	$\mathbb{P}_2$ (np=12)	
Problem size	$\mathcal{N} = 207\ 845$	$\mathcal{N} = 1\ 580\ 932$		$N = 10$
t_{exec}	6.883 s	101.81 s	21.11 s	6.27×10^{-5} s
relative time	14.8	1	35.59	1.62×10^{7}

Table 3: Times of execution for assembly + resolution of the problem

Error bound

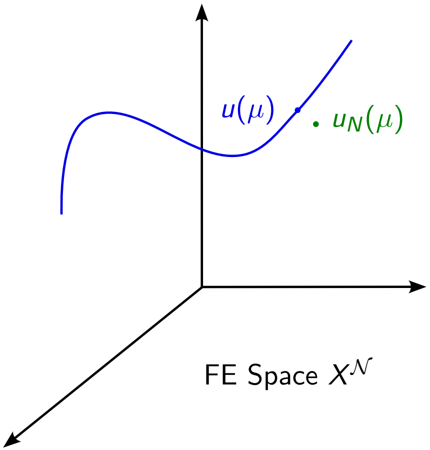

Error bound

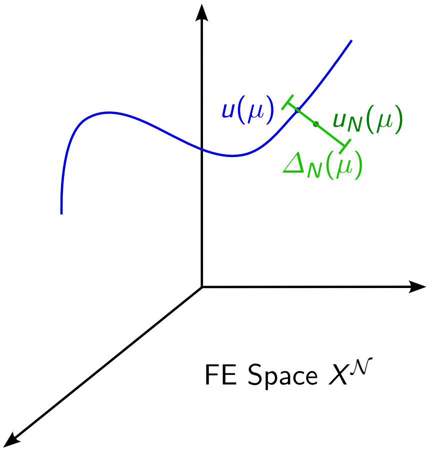

Norm of the residual error

$$\hat{e}(\mu) = \sum_p \beta_F^p(\mu)\boldsymbol{\mathcal{S}}^p + \sum_q \sum_n \beta_A^q(\mu) u_N^n(\mu) \boldsymbol{\mathcal{L}}^{n,q}$$

with :

$$\begin{aligned} (\mathcal{S}^p, v) &= f^p(v) & \forall v \in X, \forall p \in [\![1, Q_F]\!] \\ (\mathcal{L}^{n,q}, v) &= -a^q(\zeta^n, v) & \forall v \in X, \forall n \in [\![1, N]\!], \forall q \in [\![1, Q_A]\!] \end{aligned}$$

Norm of the residual error

$$\|\widehat{e}(\mu)\|_X^2 = (\widehat{e}(\mu), \widehat{e}(\mu))_X$$
$$= \left(\sum_p \beta_F^p \boldsymbol{\mathcal{S}}^p + \sum_q \sum_n \beta_A^q u_{N,n} \boldsymbol{\mathcal{L}}^{n,q}, \sum_p \beta_F^p \boldsymbol{\mathcal{S}}^p + \sum_q \sum_n \beta_A^q u_{N,n} \boldsymbol{\mathcal{L}}^{n,q} \right)_X$$

$$\|\widehat{e}(\mu)\|_X^2 = \sum_p \sum_{p'} \beta_F^p \beta_F^{p'} (\boldsymbol{\mathcal{S}}^p, \boldsymbol{\mathcal{S}}^{p'})_X + 2 \sum_p \sum_q \sum_n \beta_F^p \beta_A^q u_{N,n} (\boldsymbol{\mathcal{S}}^p, \boldsymbol{\mathcal{L}}^{n,q})_X$$
$$+ \sum_q \sum_n \sum_{q'} \sum_{n'} \beta_A^q \beta_A^{q'} u_{N,n} u_N^{n'} (\boldsymbol{\mathcal{L}}^{n',q'}, \boldsymbol{\mathcal{L}}^{n,q})_X$$

Greedy algorithm

Algorithm 1: Greedy algorithm

Input: $\mu_0 \in D^\mu$ and $\Xi_{\text{train}} \subset D^\mu$

$S \leftarrow [\mu_0]$

while $\Delta_N^{max} > \varepsilon$ **do**

  $\mu^\star \leftarrow \arg\max_{\mu \in \Xi_{\text{train}}} \|\Delta_N(\mu)\|_V^2$ (and $\Delta_N^{\text{max}} \leftarrow \max_{\mu \in \Xi_{\text{train}}} \Delta_N(\mu)$)

  Append $\mu^\star$ to S

  $u(\mu^\star) \leftarrow$ FE solution, using S as generating sample

  $\mathbb{Z}_N \leftarrow \{\boldsymbol{\xi} = \boldsymbol{u}(\mu^\star)\} \cup \mathbb{Z}_{N-1}$

end

Output: sample S, reduced basis $\mathbb{Z}_N$

Results over a sampling $\Xi_{\text{test}} \subset D^\mu$ of 100 parameters

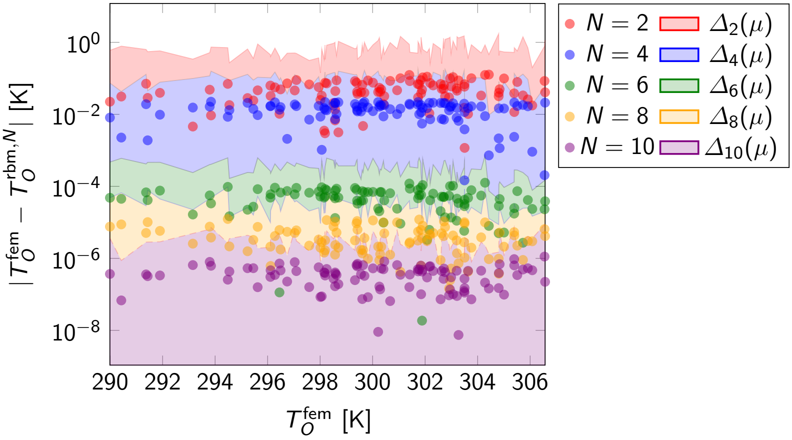

Figure 3: Error on RBM for various reduced basis sizes with error bound $\Delta_N(\mu)$

Results over a sampling $\Xi_{\text{test}} \subset D^\mu$ of 100 parameters

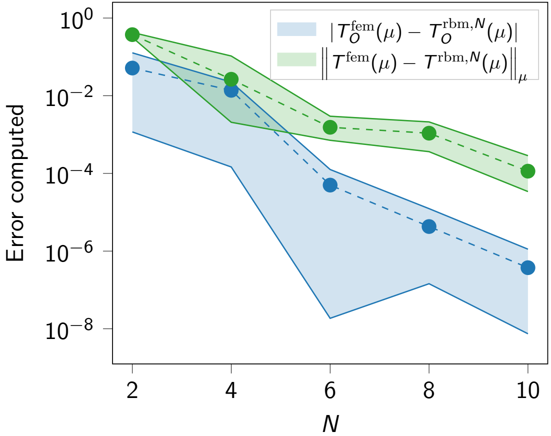

Figure 3: Convergence of the errors on the field and the output on point O

Results over a sampling $\Xi_{\text{test}} \subset D^{\mu}$ of 100 parameters

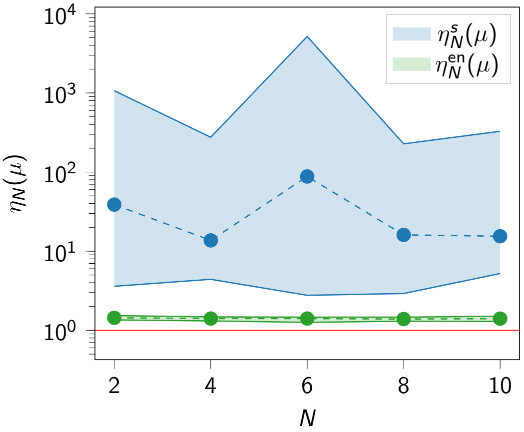

Figure 3: Stability of the effectivities $\eta_N^s(\mu)$ and $\eta_N^{en}(\mu)$

Sensitivity analysis

Sobol indices

- $\mu = (\mu_1, \dots, \mu_n) \in D^\mu$,
- $\mu_i \sim X_i$ where $(X_i)_i$ is a familly of *independent* random variables,
- Output $s_N(\mu) \sim Y = f(X_1, \dots, X_n)$,
- Distributions selected from data available in the literature.

Sobol indices

- **First-order indices**:

$$S_j = \frac{\mathrm{Var}\left(\mathbb{E}\left[Y|X_j\right]\right)}{\mathrm{Var}(Y)} \tag{1}$$

- **Total-order indices**:

$$S_j^{\text{tot}} = \frac{\mathrm{Var}\left(\mathbb{E}\left[Y|X_{(-j)}\right]\right)}{\mathrm{Var}(Y)} \tag{2}$$

where $X_{(-j)} = (X_1, \dots, X_{j-1}, X_{j+1}, \dots, X_n)$.

Distributions

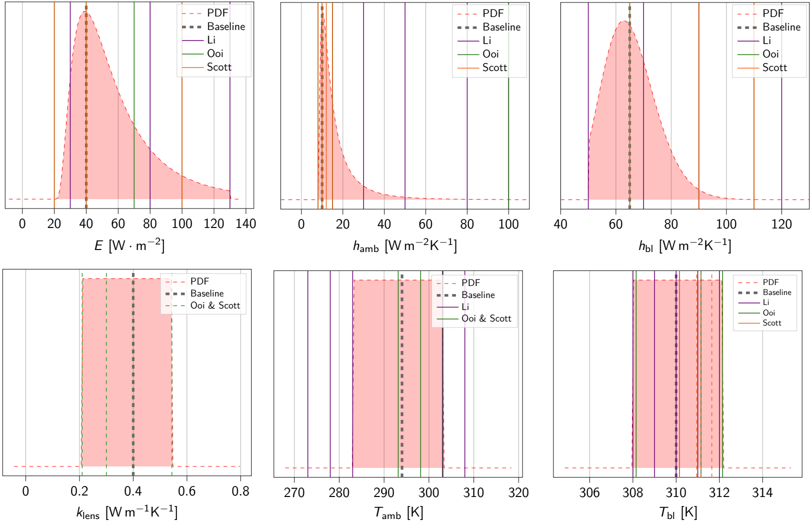

Stochastic sensitivity analysis

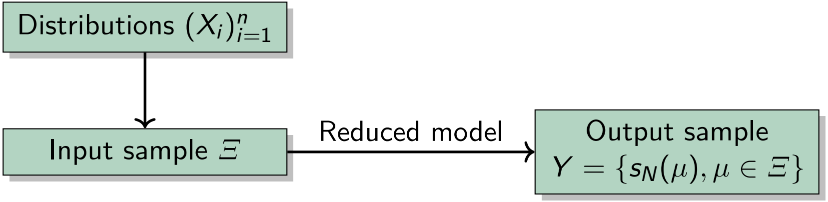

[3] Michaël Baudin et al. "OpenTURNS: An Industrial Software for Uncertainty Quantification in Simulation". In: *Handbook of Uncertainty Quantification*. Ed. by Roger Ghanem et al. Cham: Springer International Publishing, 2016, pp. 1–38.

Stochastic sensitivity analysis

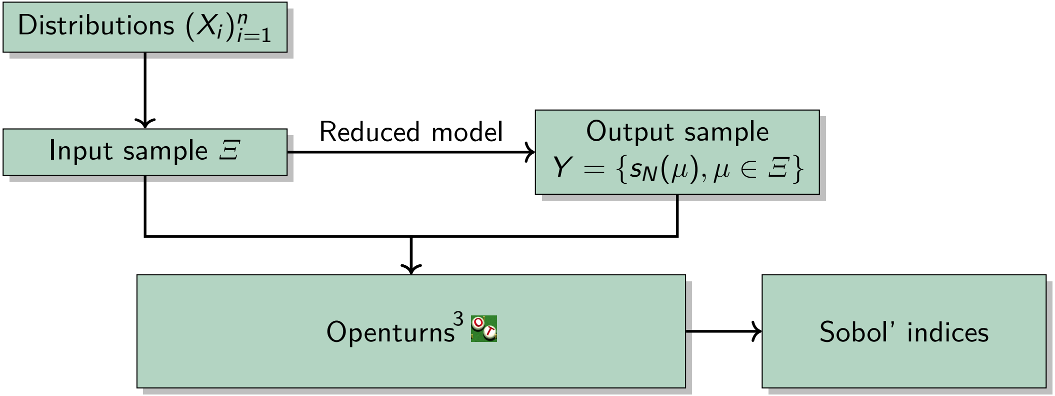

[3] Michaël Baudin et al. "OpenTURNS: An Industrial Software for Uncertainty Quantification in Simulation". In: *Handbook of Uncertainty Quantification*. Ed. by Roger Ghanem et al. Cham: Springer International Publishing, 2016, pp. 1–38.

Stochastic sensitivity analysis

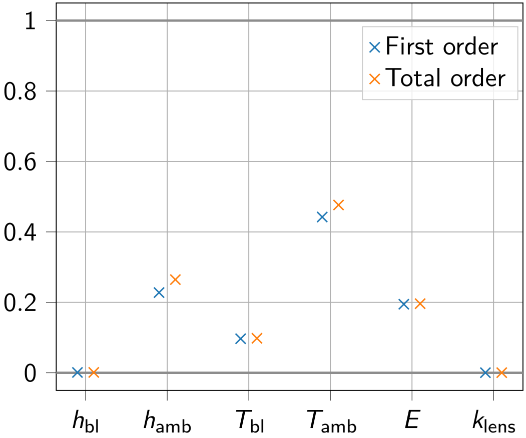

Figure 4: Sobol indices for the SSA : temperature at point O

Stochastic sensitivity analysis

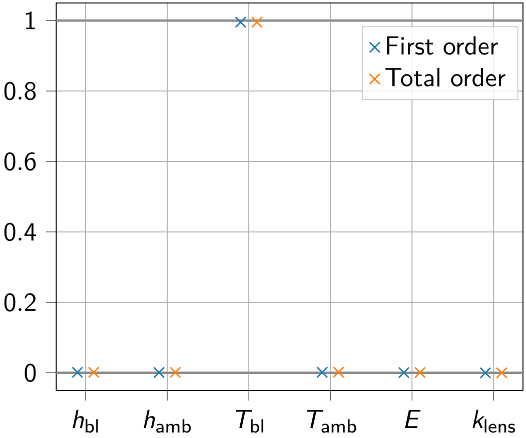

Figure 4: Temperature at point G

Conclusion and outlooks

- **Heat transport** model in the human eye :
  - FEM simulations,
  - validation against experimental data,
  - model order reduction with *certified* error bound.
- **Sensitivity analysis :**
  - **Stochastic** approach : computation of Sobol indices thanks to MOR, highlight of the impact of T_{amb} and h_{amb} on T_O. k_{lens} has not impact on any output an can be removed from the parameteric model.

Conclusion and outlooks

Next steps :

- **Model** : couple thermal effect with aqueous humor dynamics in the anterior chamber,
- **Application** : robust framework to simulate drug delivery in the eye.

What happens if we don't have access to the affine decomposition ?

Bibliography

[Bau+16] Michaël Baudin et al. "OpenTURNS: An Industrial Software for Uncertainty Quantification in Simulation". In: *Handbook of Uncertainty Quantification*. Ed. by Roger Ghanem, David Higdon, and Houman Owhadi. Cham: Springer International Publishing, 2016, pp. 1–38.

[BBS20] Ajay Bhandari, Ankit Bansal, and Niraj Sinha. "Effect of aging on heat transfer, fluid flow and drug transport in anterior human eye: A computational study". In: *Journal of Controlled Release* 328 (2020), pp. 286–303.

[Ng 06] Ng, E.Y.K. and Ooi, E.H. "FEM simulation of the eye structure with bioheat analysis". In: *Computer Methods and Programs in Biomedicine* 82.3 (2006), pp. 268–276.

[Pru+01] C. Prud'homme et al. "Reliable Real-Time Solution of Parametrized Partial Differential Equations: Reduced-Basis Output Bound Methods ". In: *Journal of Fluids Engineering* 124.1 (Nov. 2001), pp. 70–80.

Bibliography

[PW05] Christine Purslow and James S Wolffsohn. "Ocular surface temperature: a review". en. In: *Eye Contact Lens* 31.3 (May 2005), pp. 117–123.

[QMN16] Alfio Quarteroni, Andrea Manzoni, and Federico Negri. *Reduced Basis Methods for Partial Differential Equations*. Springer International Publishing, 2016.

[RF77] Robert F. Rosenbluth and Irving Fatt. "Temperature measurements in the eye". In: *Experimental Eye Research* 25.4 (1977), pp. 325–341.

[Sal19] Lorenzo Sala. "Mathematical modelling and simulation of ocular blood flows and their interactions". PhD Theses. Université de Strasbourg, Sept. 2019.

[Sco88] J.A. Scott. "A finite element model of heat transport in the human eye". In: *Physics in Medicine and Biology* 33.2 (1988), pp. 227–242.

Thank you for your attention!